ISSN 1063-7834, Physics of the Solid State, 2013, Vol. 55, No. 9, pp. 1976–1983. © Pleiades Publishing, Ltd., 2013.
Original Russian Text © A.E. Galashev, S.Yu. Dubovik, 2013, published in Fizika Tverdogo Tela, 2013, Vol. 55, No. 9, pp. 1859–1866.

GRAPHENES

Molecular Dynamics Simulation of Compression of Single-Layer Graphene

A. E. Galashev[a], * and S. Yu. Dubovik[b], **

[a] *Institute of Industrial Ecology, Ural Branch of the Russian Academy of Sciences, ul. Sofii Kovalevskoi 20, Yekaterinburg, 620219 Russia*

** e-mail: galashev@ecko.uran.ru*

[b] *Ural Federal University named after the First President of Russia B. N. Yeltsin (Ural State Technical University–UPI), ul. Mira 19, Yekaterinburg, 620002 Russia*

*** e-mail: voronina.s.u@gmail.com*

Received February 8, 2013; in final form March 5, 2013

Abstract—The compression of a single-layer graphene sheet in the "zigzag" and "armchair" directions has been investigated using the molecular dynamics method. The distributions of the *xy* and *yx* stress components are calculated for atomic chains forming the graphene sheet. A graphene sheet stands significant compressive stresses in the "zigzag" direction and retains its integrity even at a strain of ~0.35. At the same time, the stresses which accompany the compressive deformation of single-layer graphene in the "armchair" direction are more than an order in magnitude lower than corresponding characteristics for the "zigzag" direction. A compressive strain of ~0.35 in the "armchair" direction fractures the graphene sheet into two parts.

DOI: 10.1134/S1063783413090102

1. INTRODUCTION

Graphene is a two-dimensional crystal with the hexagonal structure prepared from covalently bonded carbon atoms. Owing to its unique properties, graphene is considered as a most many-sided material for application in nanotechnology. A serious disadvantage of graphene is its high brittleness. Thin graphene sheets do not stand even relatively weak compressions. Each of such deformations decreases the electrical conductivity and strength of graphene. The existence of stresses in graphene can lead to appearance of new electronic, magnetic, and kinetic properties. Thus, it is important to understand in which manner the thinnest natural membranes response on a mechanical action.

Graphene exhibits unusual mechanical properties. It demonstrates high flexibility, along with the brittleness. For example, it can be elastically expanded by ~20%. However, it conserves its brittleness in this case. The experimental studies of the mechanical properties of graphene were performed under condition of tensile and bending deformations, but compressive deformations had not been studied for a long time. However, recently, the compression of single-layer graphene was studied experimentally in [1], where a graphene sheet disposed on a plastic substrate was compressed to ~0.6% at the ratio of the length to the width of the sheet $l_{\|}/l_{\perp} > 0.2$ and to ~1% at $l_{\|}/l_{\perp} \le 0.2$. Specimens of graphene on a plastic substrate behave as perfect plates, and their behavior can be described by the Euler mechanics. It was found by transmission electron microscopy that the hydrogenation of graphene does not change the hexagonal symmetry but leads to a decrease (by ~5%) in lattice parameter *a* [2]. This fact is explained by the formation of graphane. Graphene can react with atomic hydrogen which transforms this highly conducting semimetal with a zero energy gap into a dielectric crystal—graphane. After annealing of the obtained membrane, the initial periodicity of the lattice is recovered completely.

The theory based on the standard harmonic approximation predicts the thermodynamic instability of a two-dimensional crystal, because thermal fluctuations existing in the third dimension distort the long-range order [3]. The observations in a transmission electron microscope show that the $2D$ graphene lattice can be stabilized by a weak corrugation in the third dimension [4]. The molecular dynamics simulation of compression of a single-layer graphene ribbon in the "armchair" direction shows that the ribbon deformation takes a sinusoidal character only when it does not contain vacancies [5]. The sinusoidal character of the roughness observed experimentally indicates the absence of vacancies in the deformed specimen [6]. The linear character of the stress–strain dependence is retained at low strains even when vacancies exist in the graphene ribbon. It is difficult to predict the result of the compressive deformation of the crystalline graphene considered in three-dimensional space. Such detailed theoretical studies were not performed.

The aim of this work is to study the stressed state of graphene sheet formed as a result of compressive

deformation in the "zigzag" and "armchair" directions in the framework of molecular dynamics experiment.

2. COMPUTER MODEL

The Tersoff potential used for description of interatomic interactions in graphene is based on the concept of the bond-order parameter. The potential energy between two neighboring atoms i and j is written as [7, 8]

$$V_{ij} = f_C(r_{ij})[A\exp(-\lambda^{(1)}r_{ij}) - Bb_{ij}\exp(-\lambda^{(2)}r_{ij})],$$

$$f_C(r_{ij}) = \begin{cases} 1, & r_{ij} < R^{(1)}, \\ \frac{1}{2} + \frac{1}{2}\cos[\pi(r_{ij} - R^{(1)})/(R^{(2)} - R^{(1)})], & \\ R^{(1)} < r_{ij} < R^{(2)}, & \\ 0, & r_{ij} > R^{(2)}, \end{cases}$$

where b_{ij} is the multi-particle bond-order parameter which describes how the bond formation energy (attractive part V_{ij}) is created at local atomic arrangement due to the presence of other neighboring atoms. The potential energy is a multi-particle function of positions of atoms i, j, and k and is determined by parameters

$$b_{ij} = (1 + \beta^n \xi_{ij}^{n_i})^{-1/(2n)},$$

$$\xi_{ij} = \sum_{k \neq i,j} f_C(r_{ij}) g(\theta_{ijk}),$$

$$g(\theta) = 1 + \frac{c^2}{d^2} - \frac{c^2}{[d^2 + (h - \cos\theta)^2]},$$

where ξ is the effective coordination number, $g(\theta)$ is a function of the angle between r_{ij} and r_{ik} which stabilizes the tetrahedral structure. The Tersoff potential parameters are given in table. The Tersoff potential is widely used for simulating systems with covalent bonds [9–11] and well describes many carbon forms, among them graphite [12].

We simulated a rectangular 3.4 × 3.0-nm graphene sheet (14 atoms was along each of edges) at $T = 300$ K. Its thickness was taken to be 0.142 nm. The compressive deformation was generated by displacement of two edge atomic rows of the opposite sheet edges toward to one another by 0.001 nm. Thus, each of the compression acts was characterized by the relative deformation of 0.0058 in direction of axis 0x and 0.0066 in the 0y direction. Then, we carried out a structural relaxation for 20 ps that consisted of the MD calculations of two types. In the first calculation whose time was 18 ps, the atoms of two edge rows of the opposite sheet edges used to generate the deformation

Parameters of the Tersoff potential for carbon

Parameters	Carbon [13]
A, eV	1.3936×10^3
B, eV	3.4674×10^2
$\lambda^{(1)}$, Å^{-1}	3.4879
$\lambda^{(2)}$, Å^{-1}	2.2119
β	1.5724×10^{-7}
n	7.2751×10^{-1}
c	3.8049×10^4
d	4.384
h	−0.57058
$R^{(1)}$, Å	1.8
$R^{(2)}$, Å	2.1

did not participate in thermal motion. It allowed other atoms to be rearranged according to the stresses existing in the sheet. In the second case, all the atoms took part in thermal motion, which allowed the removal of exceed stress at the sheet edges and allowed to the atoms of edge rows to occupy energetically more preferable positions. The first displacement of the opposite edges of the graphene sheet toward to one another was performed after 20 ps from starting the calculation. The calculations were performed using the Berendsen thermostat [13].

To calculate the stresses induced in graphene, the graphene sheet was divided into elementary areas. The atomic stresses $\sigma_J^i(n)$ in the nth elementary area for each of directions x, y, and z with a current index J are determined by calculating the atomic kinetic energies at this area and projections of forces f_J^i acting on the nth area from all other atoms

$$\sigma_J^i(n) = \frac{1}{k}\left\langle \sum_i^k \frac{1}{\Omega}(m v_J^i v_J^i) \right\rangle + \frac{1}{S_n}\left\langle \sum_i^k (f_J^i) \right\rangle,$$

where k is the number of atoms at the nth area; Ω is the volume per atom; m is the atomic mass; v_J^i is the Jth velocity projection of atom i; and S_n is the area of the nth area. Angular brackets indicate the averaging over time. In this case, the compressive stresses can have plus and minus signs, according to directions of forces f_J^i. In this regard, microscopic stress $\sigma_J^i(n)$ differs from macroscopic stress $\bar{\sigma}_J < 0$.

This model of perfect undeformed graphene at $T = 300$ K is characterized by the total energy −7.02 eV, which agrees well with the quantum-mechanics calculations (−6.98 eV) [14].

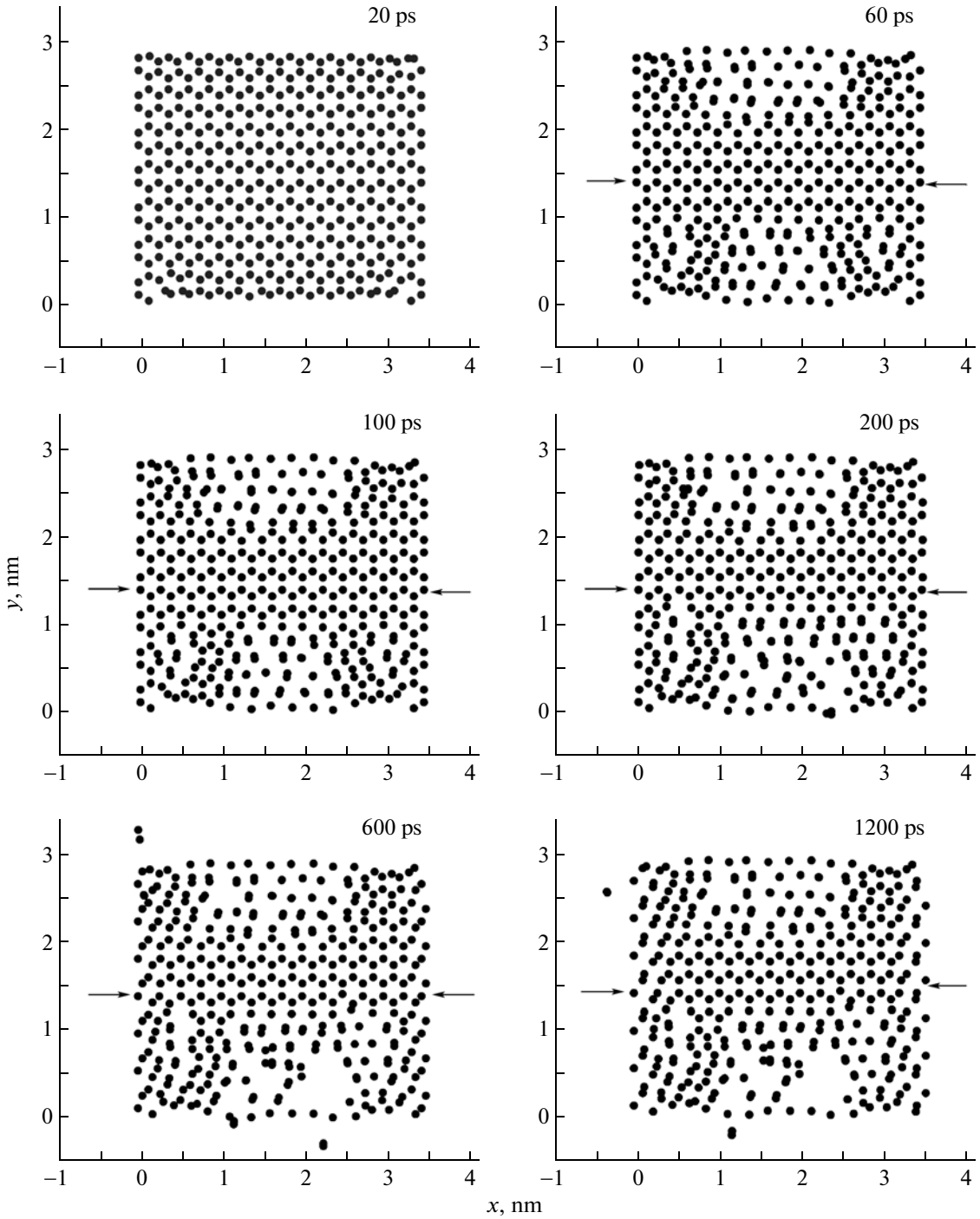

Fig. 1. Graphene sheet projection on the *xy* plane during its compression along the "zigzag" direction. The instants of time 20, 60, 100, 200, 600, and 1200 ps are characterized by the compressive strains of 0, 0.0117, 0.0235, 0.0529, 0.1705, and 0.3469, respectively. The arrows indicate the compression direction.

3. RESULTS OF THE SIMULATION

A successive compression of the graphene sheet in the "zigzag" direction (along axis 0*x*) is shown in Fig. 1. Initially, the decrease in the sheet size in the *x* direction leads to disturbance of the cellular structure in the top and bottom sheet parts to a depth on an order of two maximal cell sizes. In this case, the cellular structure of the sheet is retained from the left and right edges to approximately the same depth.

The transformation of the structure of the top and bottom regions of the sheet middle causes its transverse broadening. The broadening is maximal in the

sheet middle part and decreases when going from the middle to both left and right sides. With increasing the deformation, the fracture zone of honeycombs moves deep to the sheet (up and down), and, then, to the left and the right. To the instant of time 60 ps (at the relative deformation $\varepsilon = 0.0117$), individual atoms pressed out from the graphene sheet up and down. At very large deformations (to the instant of time 1.2 ns), the cabined graphene atoms of the left and right sheet edges are rearranged to a significant degree and even can evaporate.

It is seen from the zx projections of graphene atom coordinates that atoms begin to go out from the sheet in the z direction even at deformation $\varepsilon = 0.0235$, i.e., to the instant of time 100 ps. During further pressing the sheet, the number of atomic displacements in the z direction, as well as the distances to which atoms pass in this direction, increase.

The graphene sheet compression along the "zigzag' direction is accompanied by appearance of compressive forces acting in the $0x$ direction. Because of this, of the first interest is the distribution of stresses σ_{yx} during atomic displacement along axis $0y$ (Fig. 2). In the absence of compressive forces, dependence $\sigma_{yx}(y)$ is almost linear. After two-fold application of the compression procedure ($\varepsilon = 0.0117$), stresses of one and another signs are induced in atomic layers (to 7 levels) at the graphene sheet edges. After four-fold compression ($\varepsilon = 0.0235$), i.e., to the instant of time of 100 ps, the central straight-line segment of distribution $\sigma_{yx}(y)$ is narrowed. At the same time, the edge segments subjected to significant stresses are expanded. However, as a result of the structural relaxation, the difference in the stresses between edge atomic layers is smaller in this case, than after 60 ps ($\varepsilon = 0.0117$). The profile of $\sigma_{yx}(y)$ is changed significantly to the instant of time 200 ps ($\varepsilon = 0.0529$). In this case, the highest (for all time of the computer experiment) negative stresses are induced at the bottom sheet side. Here, we still can separate a narrow (from ~6 atomic layers) unloaded strip in the sheet middle. The stresses on the top sheet side are significantly lower than on the bottom sheet side. Due to the structural relaxation, uniformly oscillating distribution $\sigma_{yx}(y)$ is stated to the instant of time 600 ps ($\varepsilon = 0.1705$); the oscillations to be stronger at the edges, particularly, on the bottom side. Almost the same distribution $\sigma_{yx}(y)$ is retained for doubled times. However, in this case, the number of stronger oscillations of the quantity σ_{yx} in the bottom sheet part increases. The maximum oscillations of σ_{yx} take place at the instant of time 200 ps. When compressing the graphene sheet along axis $0x$, stresses σ_{yx} generate stresses σ_{xy}. Because of this, quite strong edge oscillations of σ_{xy} occur to the instant of time 600 ps. Their amplitude is maximal to the instant of time 1.2 ns ($\varepsilon = 0.3469$), in particular, at large y, where the amplitude oscillations of σ_{xy} are comparable to the amplitude variations of σ_{yx} at the instant 200 ps.

The compression along the "armchair" direction follows completely another scenario. The initial compression of the sheet leads to a flexure of the top and bottom sheet boundaries (Fig. 3) and to occurrence of transverse cracks at its lateral left and right sides. In this case, the middle part of the sheet still conserves the honeycomb structure. Further compression (to instant of time 200 ps) gives two longitudinal cracks propagating through whole graphene sheet. The zigzag-shaped honeycomb structure is retained between the cracks. The compressive stresses fracture the graphene sheet into two parts to the instant of time 600 ps. Each of the parts is broken into fragments rotated to each other at some angles. The fragments of the left sheet part are rotated at larger angles than those of the right part. Such picture is also retained, as a whole, at stronger compression (to the instant of time 1.2 ns); in this case, the gap between the left and right graphene sheet parts increases.

The emergence of atoms from the xy plane is observed in the projection of the atomic coordinates on plane xz. In this case, atoms begin to displace markedly only at deformation $\varepsilon = 0.0266$, i.e., to the instant of time 100 ps. To the instant of time 200 ps, the xz projection of the graphene sheet has even a wavy profile on the both sides of plane $z = 0$. To the instant of time 600 ps and later, the profile has even a complex form which indicates various roughness of the graphene sheet.

When the graphene sheet is compressed along the "armchair" direction, compressive forces act along the $0y$ direction. Because of this, the first-degree role is played by stresses σ_{xy} and their distribution along axis $0x$ (Fig. 4). Stresses σ_{yx} are induced as derivatives of stresses σ_{xy}. The higher resolution as compared to the case of constructing the $\sigma_{yx}(y)$ distribution makes it possible to reveal slight oscillations in the $\sigma_{xy}(y)$ distribution even at the absence compressive deformation. Here, the right-side edge (large x) is more unloaded than the left-side edge. After two-fold compression ($\varepsilon = 0.0133$), the stresses from the left and right sides of the sheet are changed more substantially than in the sheet middle. With time, substantial changes in the stresses shift to the sheet middle. Stresses σ_{xy} form most high jump in adjacent atomic layers at the instant 100 ps, when $\varepsilon = 0.0266$. To the instant of time 200 ps, the character of the distributions of stresses σ_{xy} is changed substantially. On the left side, a quite monotonic decreasing segment of function $\sigma_{xy}(x)$ forms. The right side of the $\sigma_{xy}(x)$ distribution is a slightly oscillating flat segment with significant decrease in the edge value of the function. To the instant of 600 ps, the $\sigma_{xy}(x)$ distribution takes a more uniform oscillating form, the elongated oscillations of which become higher and sharper to the instant 1.2 ns ($\varepsilon = 0.3929$). It is remarkable that the largest oscillation amplitude of function $\sigma_{xy}(x)$ observed at the instant 100 ps is substantially smaller (by a factor of

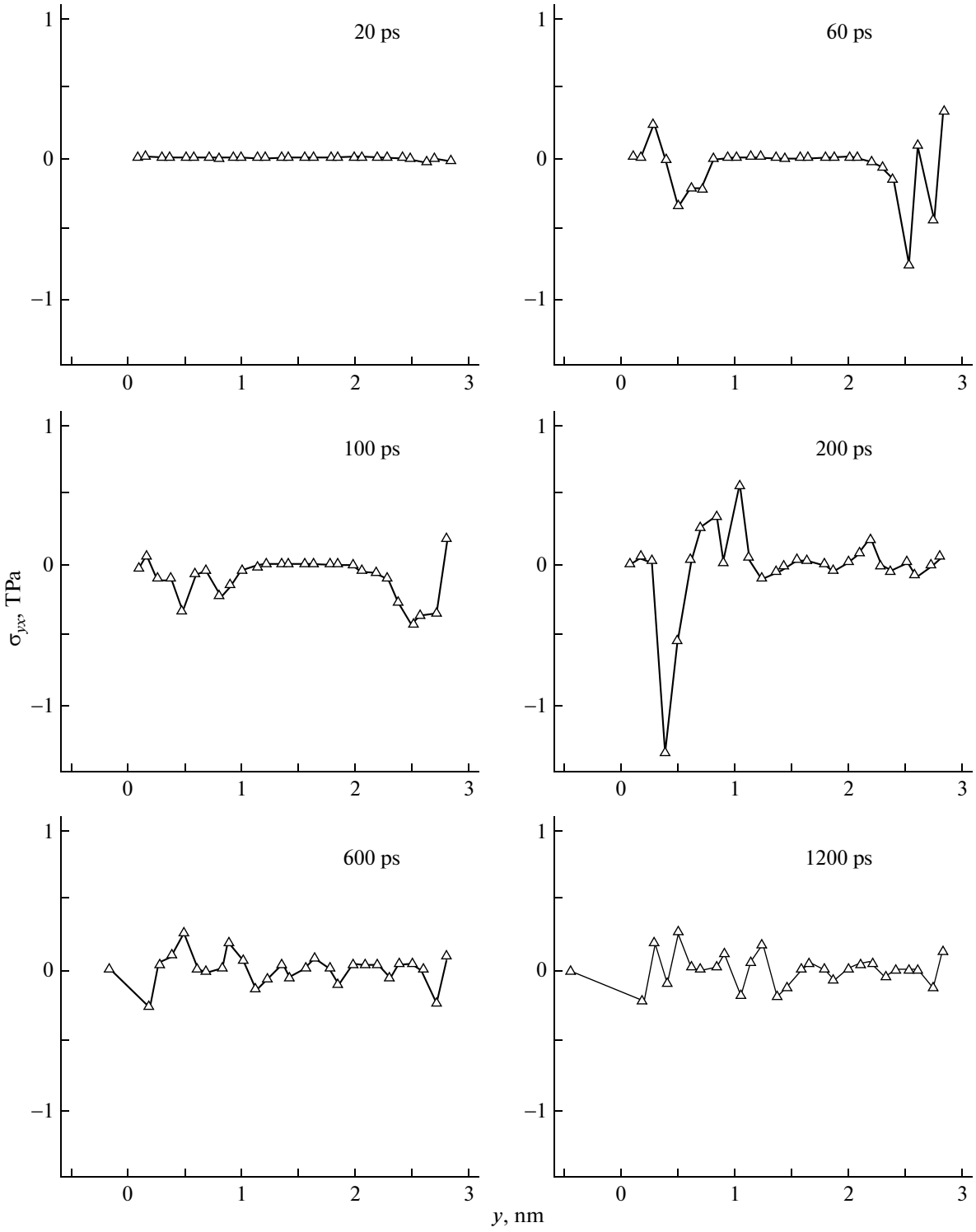

Fig. 2. Distribution $\sigma_{yx}(y)$ of the stress tensor component of the graphene sheet along the "armchair" direction for six instants of time at the compressive "zigzag" strains of 0.0117, 0.0235, 0.0529, 0.1705, and 0.3469.

14.5) than similar characteristic of function $\sigma_{yx}(y)$ observed at the instant 200 ps during compressing along the "zigzag" direction. In the case of compression along the "armchair" direction, the largest oscillation amplitude of function $\sigma_{yx}(y)$ observed at the instants of 60 and 200 ps is not higher than 50% of corresponding value for distribution $\sigma_{xy}(x)$ during compression along the same direction.

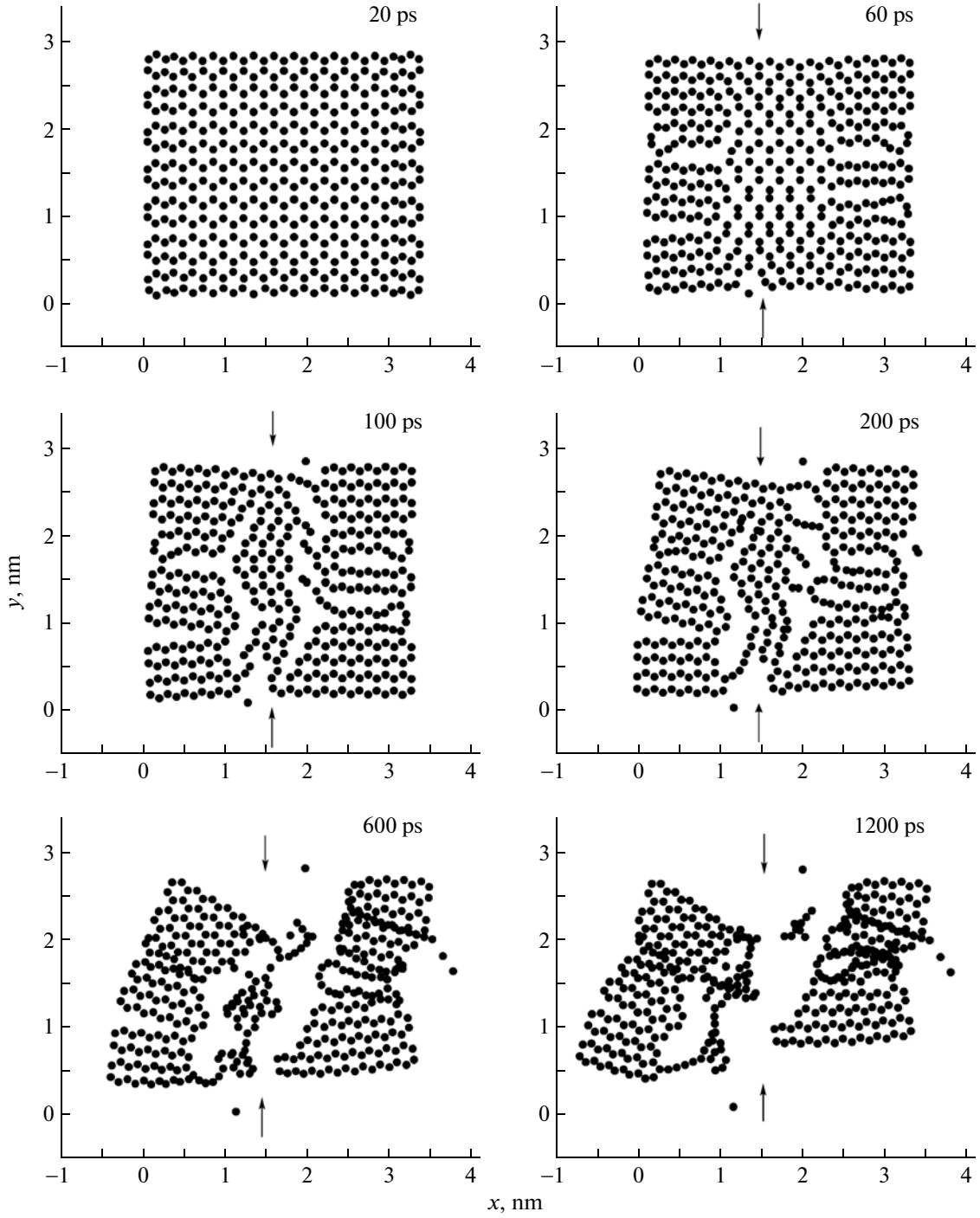

Fig. 3. Graphene sheet projection on the *xy* plane during its compression along the "armchair" direction. The instants of time 20, 60, 100, 200, 600, and 1200 ps are characterized by the compressive strains of 0, 0.0133, 0.0266, 0.0599, 0.1931, and 0.3929, respectively. The arrows indicate the compression direction.

In the MD study [15], where the Tersoff–Brenner potential [8, 16] was used, the data on the critical stresses and tensile deformations of a perfect graphene sheet were obtained as follows: 123 GPa and 23.3%, respectively for the longitudinal mode ("zigzag" direction) and 127 GPa and 21.84%, respectively, for the transverse mode ("armchair" direction). Assuming that the state of the compressed graphene sheet, in which the difference between stresses in atomic layers is maximal, is a critical state, we obtain, using the date of this study, the values –31.5 GPa and 5.3% for compression along the "zigzag" direction and –2.2 GPa

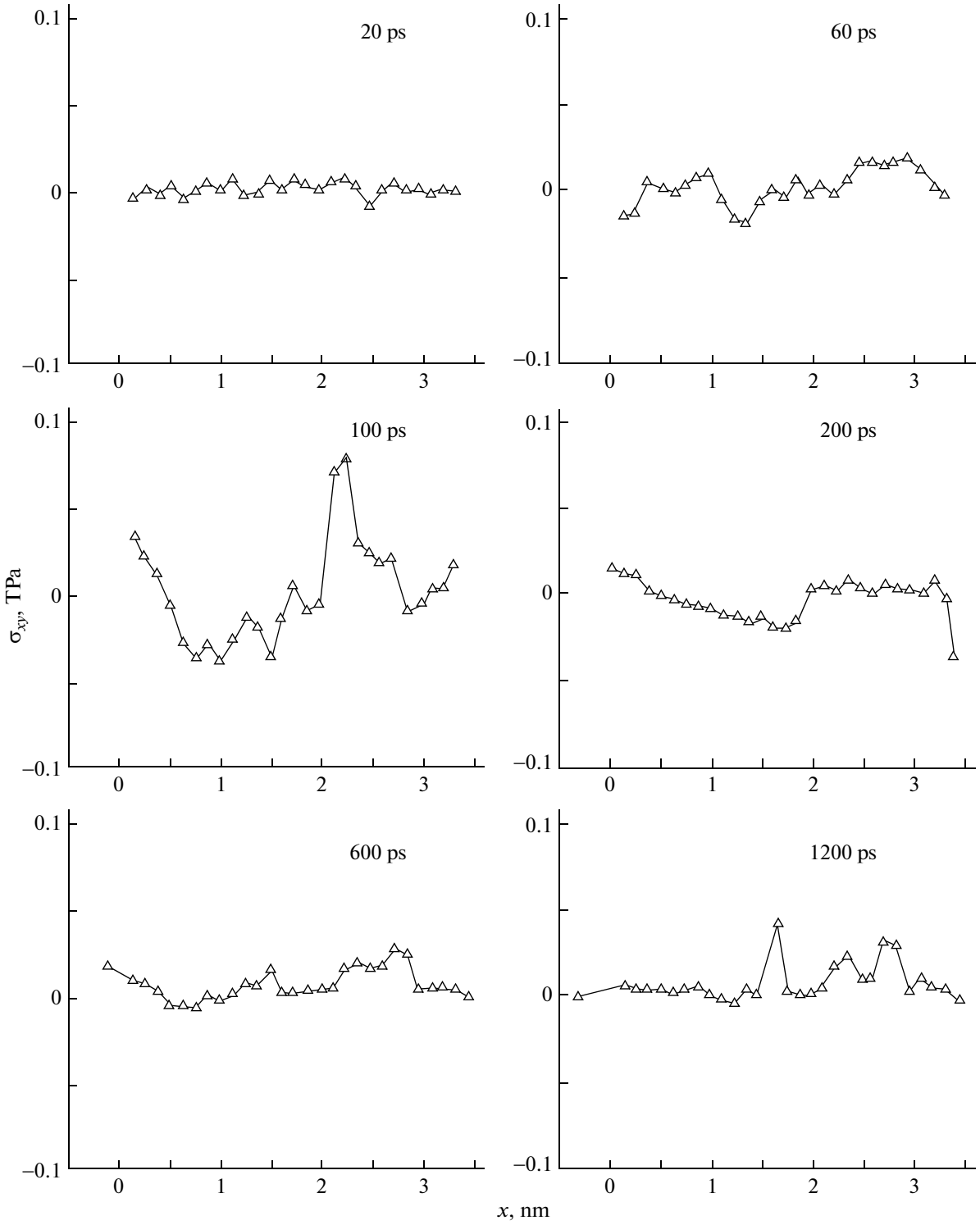

Fig. 4. Distribution $\sigma_{xy}(x)$ of the stress tensor component of the graphene sheet along the "zigzag" direction for six instants of time at the compressive "armchair" strains of 0, 0.0133, 0.0266, 0.0599, 0.1931, and 0.3929.

and 2.6% for compression along the "armchair" direction. Here, the average critical stress is determined as the sum of forces acting to individual areas at corresponding instant of time divided by the sheet surface area.

4. CONCLUSIONS

The compressive deformation of graphene sheet in the "zigzag" and "armchair" directions has been studied using the molecular-dynamic model. It is found

that the graphene sheet behaves principally differently at these strains. The compression in the "zigzag" direction weakens the sheet edges parallel to this direction because of local fracture of cellular hexagonal structure along the bottom and top sheet edges. As a result, after 59 compression acts by $\varepsilon = 0.0058$, the graphene sheet retains its integrity and loses only a small number of C atoms. The defect cellular structure is conserved in the *H* form. The graphene sheet cannot stand such high stresses in the "armchair" direction. Compression of the graphene sheet in the "armchair" direction even at small strains leads to the formation of cracks along the "zigzag" direction. Then, because of these cracks, convoluted channels are formed in the "armchair" direction. Further compression leads to rotation of individual graphene sheet fragments and displacement of the left-side sheet part with respect to the right-side part. In this case, one of the formed channels is expanded. The rotated left and right sheet parts slide along this channel, and, as a result, the sheet is completely fractured. In this case, the difference in stresses in atomic layers of the graphene sheet is smaller by more than an order of magnitude than the corresponding characteristic observed when the sheet is compressed along the "zigzag" direction.

REFERENCES

1. O. Frank, G. Tsoukleri, J. Parthenios, K. Papagelis, I. Riaz, R. Jalil, K. S. Novoselov, and C. Galiotis, ACS Nano **4**, 3131 (2010).
2. J. O. Sofo, A. S. Chaudhari, and G. D. Barber, Phys. Rev. B: Condens. Matter **75**, 153401 (2007).
3. L. D. Landau and E. M. Lifshitz, *Course of Theoretical Physics*, Vol. 5: *Statistical Physics, Part 1* (Nauka, Moscow, 1976; Butterworth–Heinemann, Oxford, 1980).
4. J. C. Meyer, A. K. Geim, M. I. Katsnelson, K. S. Novoselov, T. J. Booth, and S. Roth, Nature (London) **46**, 7131 (2007).
5. M. Neek-Amal and F. M. Peeters, Appl. Phys. Lett. **97**, 153118 (2010).
6. W. Bao, F. Miao, Z. Chen, H. Zhang, W. Jang, C. Dames, and C. Ning Lau, Nat. Nanotechnol. **4**, 562 (2009).
7. J. Tersoff, Phys. Rev. Lett. **61**, 2879 (1988).
8. J. Tersoff, Phys. Rev. B: Condens. Matter **37**, 6991 (1988).
9. D. B. Boercker, Phys. Rev. B: Condens. Matter **44**, 11592 (1991).
10. A. Y. Galashev, Mol. Phys. **107**, 2555 (2009).
11. A.Y. Galashev, J. Nanopart. Res. **12**, 3003 (2010).
12. K. Nordlund and J. Keinonen, Phys Rev. Lett. **77**, 699 (1996).
13. H. J. C. Berendsen, J. P. M. Postma, W. F. van Gunsteren, A. Di Nola, and J. R. Haak, J. Chem. Phys. **81**, 3684 (1984).
14. S. Yu. Davydov, Phys. Solid State **54** (4), 875 (2012).
15. R. Ansari, S. Ajori, and B. Motevalli, Superlattices Microstruct. **51**, 274 (2012).
16. D. W. Brenner, Phys. Rev. B: Condens. Matter **42**, 9458 (1990).

Translated by Yu. Ryzhkov